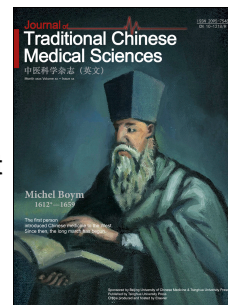


# Accepted Manuscript

Identification of berbamine dihydrochloride from barberry as an anti-adipogenic agent by high-content imaging assay

Shifeng Wang, Qiao Zhang, Yuxin Zhang, Yanling Zhang, Qinghua Wu, Shiyu Li, Yanjiang Qiao



PII: S2095-7548(16)30015-1

DOI: [10.1016/j.jtcms.2016.07.007](https://doi.org/10.1016/j.jtcms.2016.07.007)

Reference: JTCMS 74

To appear in: *Journal of Traditional Chinese Medical Sciences*

Received Date: 1 March 2016

Accepted Date: 12 July 2016

Please cite this article as: Wang S, Zhang Q, Zhang Y, Zhang Y, Wu Q, Li S, Qiao Y, Identification of berbamine dihydrochloride from barberry as an anti-adipogenic agent by high-content imaging assay, *Journal of Traditional Chinese Medical Sciences* (2016), doi: 10.1016/j.jtcms.2016.07.007.

This is a PDF file of an unedited manuscript that has been accepted for publication. As a service to our customers we are providing this early version of the manuscript. The manuscript will undergo copyediting, typesetting, and review of the resulting proof before it is published in its final form. Please note that during the production process errors may be discovered which could affect the content, and all legal disclaimers that apply to the journal pertain.

**Identification of berbamine dihydrochloride from barberry as an anti-adipogenic agent by high-content imaging assay**

Shifeng Wang<sup>a</sup>, Qiao Zhang<sup>a</sup>, Yuxin Zhang<sup>a</sup>, Yanling Zhang<sup>a</sup>, Qinghua Wu<sup>b</sup>,  
Shiyu Li<sup>c,\*</sup>, Yanjiang Qiao<sup>a,\*</sup>

<sup>a</sup>School of Chinese Materia Medica, Beijing University of Chinese Medicine,  
Beijing 100102, China

<sup>b</sup>HD Biosciences Co., Ltd., Shanghai 201201, China

<sup>c</sup>Key Laboratory of Genomic and Precision Medicine, Beijing Institute of  
Genomics, Chinese Academy of Sciences, 1 Beichen West Road, Chaoyang  
District, Beijing 100101, China

**\*Corresponding authors**

Tel.: +86-10-8049-7628, Fax: +86-10-8049-7628,

E-mail: lishiyu@big.ac.cn (S. Li)

Tel.: +86-10-8473-8620, Fax: +86-10-8473-8661,

E-mail: yjqiao@bucm.edu.cn (Y. Qiao)

**Abstract**

*Objective:* Lipid droplet (LD) deposition in adipose tissue is a critical factor leading to metabolic dysfunction. Various herbal medicines in traditional Chinese medicine (TCM) are used to treat hyperlipidemia, type 2 diabetes, obesity, and other diseases. The objective of this study was to identify potential anti-adipogenic agents from TCM herbal compounds.

*Methods:* One hundred and twenty compounds were evaluated in terms of their effect on adipocyte differentiation through image-based high content screening. Anti-adipogenic effects of identified hits were further confirmed at various concentrations. In addition, drug-induced liver injury assay was performed with HepG2 cells to test the hepatotoxicity of hit compounds.

*Results:* Berbamine (BBM), a chemical isolated from barberry, and a derivative of BBM, berbamine dihydrochloride (BBMD), reduced LDs formation by more than 50%. Dose-dependent effects were observed and the IC<sub>50</sub> values of the two hits, BBM and BBMD, were determined as 1.88 μM and 0.95 μM, respectively. Moreover, BBM induced mild HepG2 cell injury, while its dihydrochloride—BBMD did not exhibit hepatotoxicity within 40 μM.

*Conclusion:* This study demonstrates that BBMD may be a potential therapeutic candidate for disorders associated with elevated LDs accumulation.

**Keywords**

3T3-L1 adipocyte; berbamine dihydrochloride; hepatotoxicity; high content  
screening; lipid droplet

ACCEPTED MANUSCRIPT

## Introduction

Lipid droplets (LDs) are dynamic intracellular organelles that play an important role in cellular lipid storage and trafficking.<sup>1</sup> LDs mainly contain triglycerides, the metabolic precursor diacylglycerol,<sup>2</sup> and perilipin.<sup>3</sup> Overloaded intracellular LDs are associated with metabolic diseases such as obesity, insulin resistance, non-alcoholic fatty liver disease (NAFLD), and type 2 diabetes.<sup>4</sup> Recent research by Tirinato et al.<sup>5</sup> showed that high levels of LDs were present in colorectal cancer stem cells, and may thus be a cellular target for innovative anticancer therapies. LDs are mainly stored in adipose tissue. Also, 3T3-L1 preadipocyte derived from Swiss mouse embryo tissue is a typical fat-storage cell line that differentiates into mature adipocytes when stimulated by hormone cocktail, consisted by insulin, dexamethasone, and 3-Isobutyl-1-methylxanthine (IBMX).<sup>6</sup> In research, 3T3-L1 adipocytes were used as a target for the discovery of anti-adipogenic drugs.<sup>7</sup>

Currently, there are three main approaches for quantifying LDs. The first (conventional) method, which is labor intensive and time consuming, is to use oil red O staining and signal acquisition by ultraviolet spectroscopy. The second method is a label-free method, with bright-field microscopy<sup>8</sup> and spectroscopy imaging<sup>5</sup> as examples. The third method applies lipophilic fluorescent dyes specific for neutral LDs,<sup>9</sup> which makes high-content detection of LDs in 3T3-L1 adipocytes feasible. These assays have facilitated discovery of novel anti-adipogenic ingredients.

Metabolic disorders generally require long-term intake of lipid-regulating drugs. The liver is the primary organ for both fat and drug metabolism, and is thus subjected to potential hazardous agents. Therefore, during drug development, attention must be paid to drug safety. For example, individuals with NAFLD are exposed to a high risk of drug-induced liver injury (DILI) during long-term consumption of anti-hyperlipidemia drugs.<sup>10</sup> Using drug-induced liver toxicity assays, with high sensitivity and specificity developed by high throughput format<sup>11-13</sup> is paramount for predicting the safety of the identified hits at early stage of drug discovery.

In China, many traditional herbs are prescribed for regulating lipid metabolism, such as milk thistle (*Silybum marianum* (L.) Gaertn.),<sup>14</sup> salvia root (*Salvia miltiorrhiza* Bunge), astragalus root (*Astragalus membranaceus* (Fisch.) Bunge),<sup>15</sup> cassia seed (*Senna obtusifolia* (L.) H.S.Irwin & Barneby),<sup>16</sup> and coptis rhizome (*Coptis chinensis* Franch.).<sup>17</sup> However, understanding of the molecular bioactivities of these plants remains incomplete. The aim of the present study was to screen and identify novel anti-adipogenic agents from Chinese herbs and to predict their hepatotoxicity using a high-content imaging assay.

## Materials and methods

### *Herbal compounds and reagents*

A total of 120 traditional Chinese medicine (TCM) herbal compounds with diverse chemical structures were purchased from the Beijing Institute for Drug Control (Beijing, China) and Dalian Institute of Chemical Physics (Dalian, China). The purity of all the compounds was >98%. The test compounds were derived from Chinese herbs that are commonly prescribed and are thus readily available.

Compounds were dissolved in dimethyl sulphoxide (DMSO) and immediately stored at  $-20^{\circ}\text{C}$  as a stock solution for testing. A ToxInsight™ Drug Induced Liver Injury (DILI) Cartridge was purchased from Thermo Scientific (Waltham, MA, USA). Dulbecco's modified Eagle's medium (DMEM) and fetal bovine serum (FBS) were obtained from Gibco (Grand Island, NY, USA). Dexamethasone, 3-isobutylxanthine (IBMX), lovastatin, Nile Red, Hoechst 33342, and all other chemicals were purchased from Sigma–Aldrich (Saint Louis, MO, USA), if not otherwise stated.

#### *Induction of adipogenic differentiation*

3T3-L1 pre-adipocytes (American Type Culture Collection, Manassas, VA, USA) were cultured in 10-cm dishes in DMEM supplemented with 10% FBS, 100 unit/mL penicillin, and 100  $\mu\text{g}/\text{mL}$  streptomycin. Cultures were maintained in a humidified atmosphere of 5%  $\text{CO}_2$  in air at  $37^{\circ}\text{C}$ . 3T3-L1 adipocytes differentiation was performed as reported previously.<sup>18</sup> Plating of cells was

defined as Day 1. Initiation of differentiation was conducted on Day 4, and promotion of differentiation was done on Day 6 using insulin medium (1  $\mu\text{g}/\text{mL}$ ). The differentiation medium comprised 0.5 mM IBMX, 1  $\mu\text{g}/\text{mL}$  insulin, 0.25  $\mu\text{M}$  dexamethasone, and 2  $\mu\text{M}$  rosiglitazone. Adipocytes were incubated further in DMEM complete culture medium for 2 days. For determination of the Z' factor, 30 differentiated and 30 undifferentiated wells were performed in parallel.

#### *Chemical treatment*

TCM test compounds were added to confluent 3T3-L1 pre-adipocytes from Day 3, and were continuously present for 6 days. During primary screening, 120 test compounds were prepared at a concentration of 4 mM in 100% DMSO, and then diluted into 100  $\mu\text{M}$  using DMEM complete culture medium. For dose-response titration, tested compounds were three-fold serially diluted in DMSO from 12 mM stock solutions and were further diluted into complete culture medium. Three replicates were performed in parallel for each dose.

#### *Staining and imaging of 3T3-L1 adipocytes*

By the end of cell differentiation (Day 10), culture media were removed and cells were rinsed gently with phosphate-buffered saline (PBS). First, 100  $\mu\text{L}$  of 4% paraformaldehyde solution was added to each well and the plates maintained at 25°C for 20 minutes, followed by rinsed with PBS. Next, 100  $\mu\text{L}$



of 5  $\mu\text{g}/\text{mL}$  freshly prepared Nile Red solution was applied to each well and incubated at 25°C for 10 minutes. Then Nile Red solution was removed and the plate was rinsed with PBS. Finally, 10  $\mu\text{g}/\text{mL}$  Hoechst 33342 was added to cells and kept at 25°C for 15 minutes, followed by rinsed with PBS.

Signals of lipid droplets and nuclei staining in 3T3-L1 adipocytes were captured using the imaging platform Cellomics ArrayScan<sup>®</sup> VTI HCS Reader (Thermo Scientific) with a 10 $\times$  objective lens; eight fields per well were scanned. Images were analyzed using the Cellomics Cell Health Profiling BioApplication v4 protocol (Thermo Scientific).

#### *DILI assay*

Evaluation of hepatotoxicity was conducted according to procedures described previously.<sup>18</sup> Briefly, hepatocellular carcinoma (HepG2) cells were seeded in 96-well microplates (8000 cells/well) in complete DMEM. The cells were incubated overnight at 37°C. TCM test compounds were added to cells and incubated for 24 hours. Aspirin was used as a non-toxic drug control with a maximum concentration of 554  $\mu\text{M}$  (100 $\times$  the maximum concentration in plasma ( $C_{\text{max}}$ )). Gemfibrozil (GEM) was used as a positive control at a maximum concentration of 850  $\mu\text{M}$  (100 $\times$   $C_{\text{max}}$ ). Berbamine (BBM) and berbamine dihydrochloride (BBMD) were each serially diluted twofold from 40  $\mu\text{M}$ .

### *Staining and imaging of HepG2 cells*

A ToxInsight DILI Assay Cartridge was used to simultaneously monitor cell nuclei, glutathione (GSH), reactive oxygen species (ROS), and the mitochondrial membrane potential (MMP). Imaging of live cells was achieved by addition of 100  $\mu$ L of DMEM culture medium containing four fluorescent dyes to each well. Plates were maintained at 37°C for 45 minutes. To minimize photo-bleaching, cells were gently rinsed once with Hank's balanced salt solution. Images were captured immediately on the Cellomics ArrayScan VTI HCS Reader, and analyzed using the Cellomics Compartmental Analysis v4 protocol (Thermo Scientific).

### *Statistical analyses*

Data was representative of at least three repeated experiments. Statistical analyses were done with GraphPad Prism v5.0 (GraphPad, La Jolla, CA, USA). The Student's *t*-test was used for comparison of individual groups;  $P < .05$  was considered significant. The Z' factor was calculated using the following formula<sup>19</sup>:

$$Z' = 1 - 3 \times \left\{ \frac{SD_{(\text{differentiated})} + SD_{(\text{undifferentiated})}}{\text{Mean}_{(\text{differentiated})} - \text{Mean}_{(\text{undifferentiated})}} \right\}$$

LD content was normalized to differentiated vehicle control and inhibitory percentage was determined according to the following formula:

$$\text{Inhibition (\%)} = 100 \times \frac{\text{Intensity}_{(\text{sample})} - \text{Intensity}_{(\text{undifferentiated})}}{\text{Intensity}_{(\text{differentiated})} - \text{Intensity}_{(\text{undifferentiated})}}$$

## Results

### *Anti-adipogenic assay development*

To discover novel anti-adipogenic agents from 120 TCM herbal compounds, a high-content imaging assay of adipocyte differentiation was developed. 3T3-L1 adipocytes were differentiated as described in the Materials and Methods section. Adipocytes with stained LDs were defined as differentiated cells, while adipocytes absent of LDs were defined as quiescent cells (Fig. 1A). The Z' factor represents the robustness of the assay, and was determined to be 0.63 (n = 30), and the signal/noise ratio was 11 (Fig. 1B), suggesting that the assay was feasible for high-content screening. Lovastatin was used as a positive control and a dose-dependent response was observed. The half-maximal inhibitory concentration (IC<sub>50</sub>) was 1.4 μM (Fig. 1C), which was in general agreement with IC<sub>50</sub> values reported previously.<sup>20</sup>

A

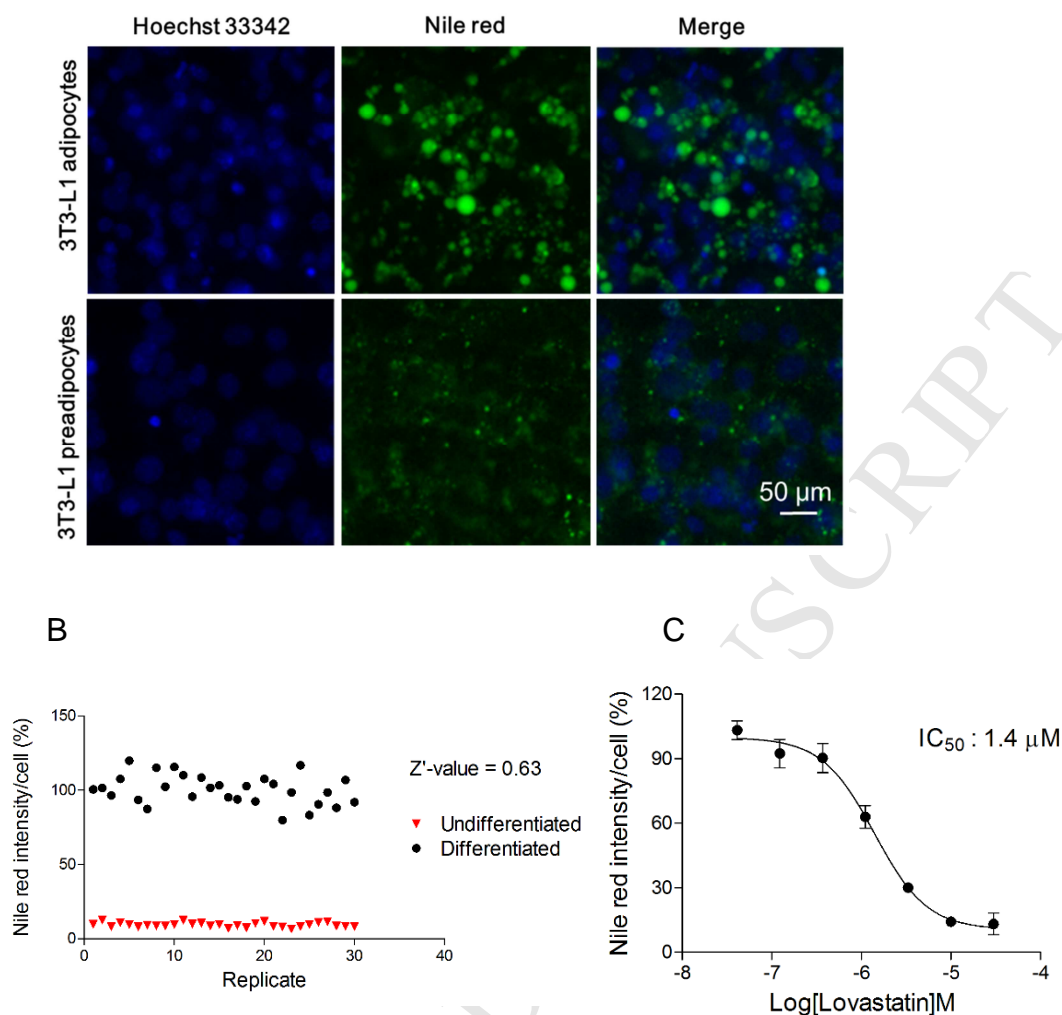


**Figure 1** High-content imaging assay

(A) Nile Red-labeled lipid droplets and Hoechst 33342-stained nuclei in 3T3-L1 pre-adipocytes and mature adipocytes. 0.25% DMSO-treated 3T3-L1 adipocytes were defined as negative controls ( $n = 6$ ). Scale bar = 50  $\mu\text{m}$ . (B) Scatter plot distribution of the percentage of lipid droplets in mature adipocytes (solid circle) and undifferentiated pre-adipocytes (solid triangle). (C) Dose–response curve of lovastatin for accumulation of lipid droplets.

*Screening for anti-adipogenic compounds*

The high-content imaging assay was applied to 120 TCM compounds. Fifty-percent inhibition was considered the cutoff criterion. BBM (Fig. 2A) and one of its derivatives, BBMD (Fig. 2B), were identified. The number and size of LDs decreased significantly ( $P < .001$ ) in BBM- and BBMD-treated adipocytes (Fig. 3A). Inhibition by BBM and BBMD attained a maximum of 90%, whereas a small cluster of compounds exhibited negative inhibition values, as illustrated by accentuation of LD accumulation in adipocytes (Fig. 3B). Viability of adipocytes was assessed by staining using Hoechst 33342. Viability of adipocytes treated by BBM or BBMD declined slightly, but the decline did not reach 50% (Fig. 3C).

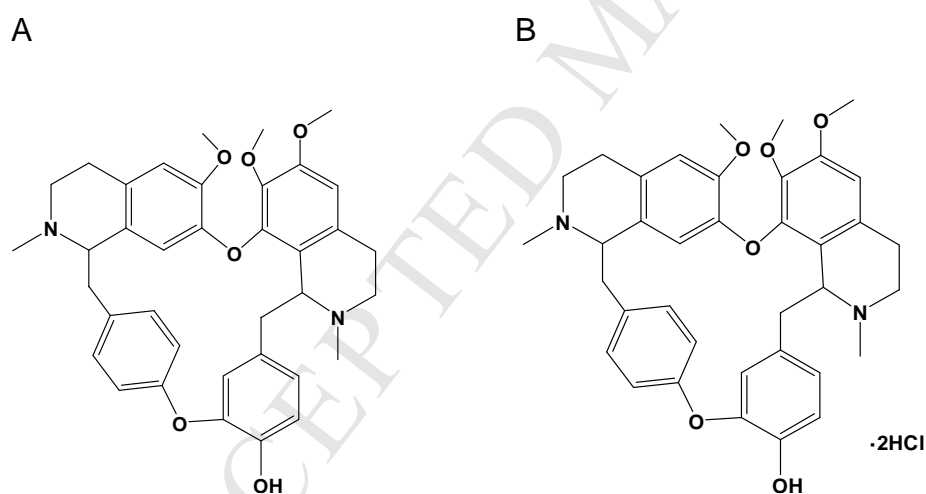


**Figure 2** Chemical structures of (A) berbamine and (B) berbamine dihydrochloride.

A

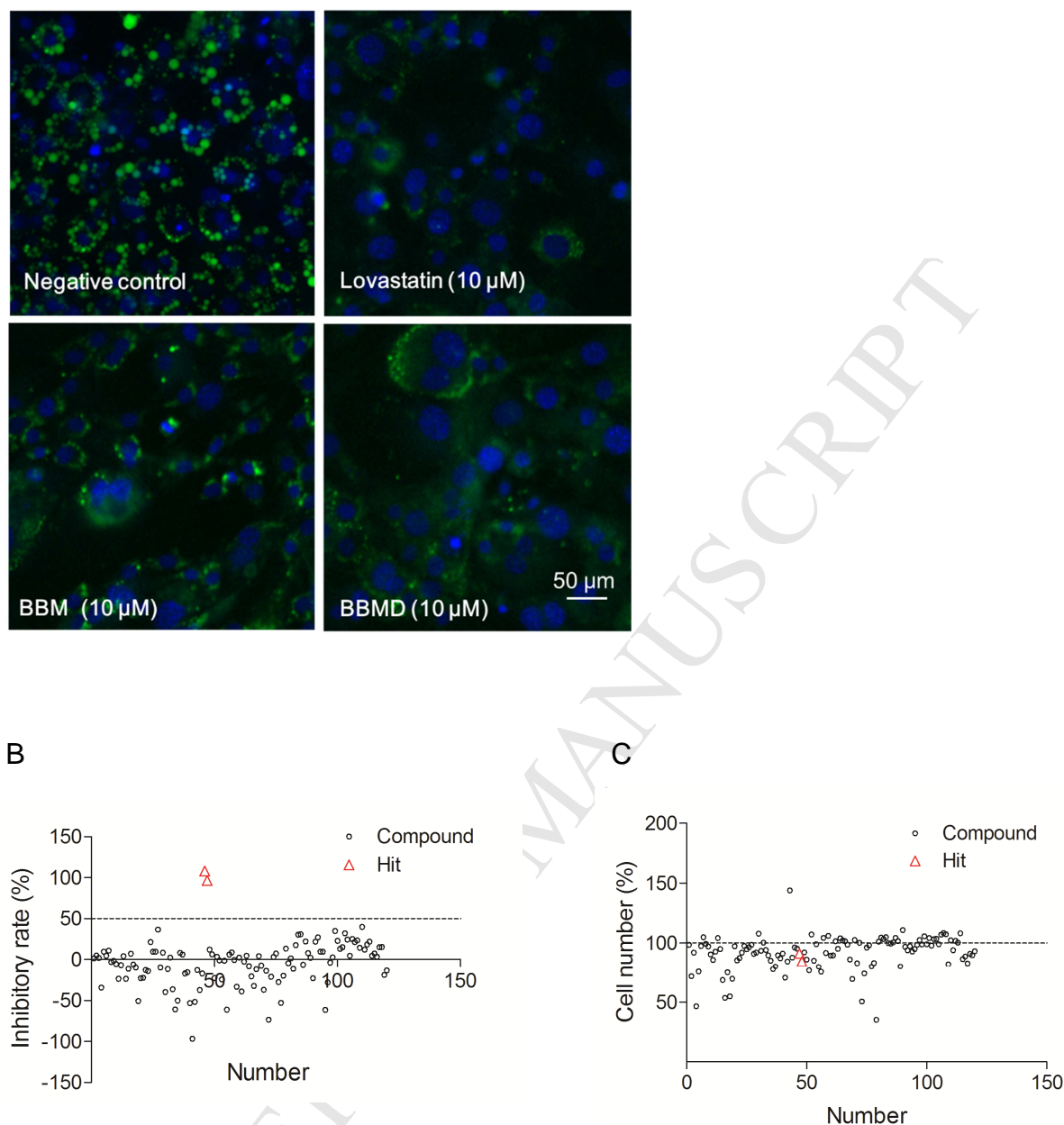


**Figure 3** Primary screening of inhibitors of the formation of lipid droplets at 10 μM.

(A) Representative images of 3T3-L1 adipocytes labeled with Nile Red and Hoechst 33342 incubated with or without a test compound. Scale bar = 50 μm. (B) Primary screening at 10 μM. 3T3-L1 pre-adipocytes were incubated in parallel in the absence of differentiation and used as blank controls. Mature adipocytes were used as negative controls and defined as 100%. (C) Viability of 3T3-L1 adipocytes treated with

test compounds; the percentage was normalized to that for the negative control. Data represent mean value of three independent experiments.

#### Confirmation of the anti-adipogenic effect of BBM and BBMD

To verify the anti-adipogenic effects of BBM and BBMD, we created dose-response curves from a maximum final concentration of 30  $\mu\text{M}$ . BBM and BBMD reduced LD deposition potently in 3T3-L1 adipocytes in a dose-dependent manner.  $\text{IC}_{50}$  values of BBM and BBMD were 1.88  $\mu\text{M}$  (Fig. 4A) and 0.95  $\mu\text{M}$  (Fig. 4B), respectively. BBM and BBMD did not influence cell viability within 10  $\mu\text{M}$ , but obvious cell losses were caused by BBM and BBMD at 30  $\mu\text{M}$  ( $P < .001$ ) (Fig. 4C). Therefore, treatment of BBM or BBMD at 10  $\mu\text{M}$  could achieve up to 80% inhibitory effect, while used at 30  $\mu\text{M}$  could induce cytotoxicity.

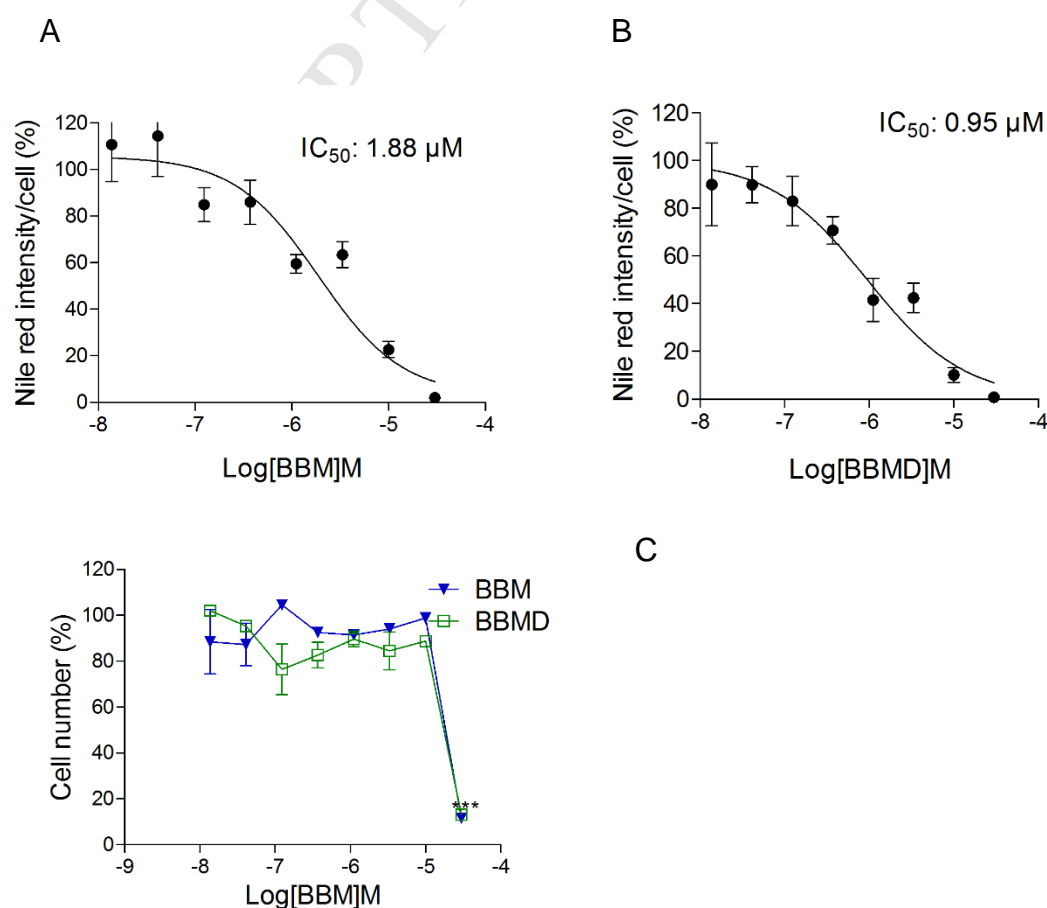


**Figure 4** Inhibitory effects of berbamine (BBM) and berbamine dihydrochloride (BBMD) on formation of lipid droplets in 3T3-L1 adipocytes.

(A) Dose–response curve of the effect of BBM on LD formation; (B) Dose–response curve of the effect of BBMD on LD formation; (C) Number of BBM- and BBMD-treated 3T3-L1 adipocytes.

All datasets were normalized to negative controls and represented as the mean (SEM),  $n = 6$ ,  $***P < 0.001$ .

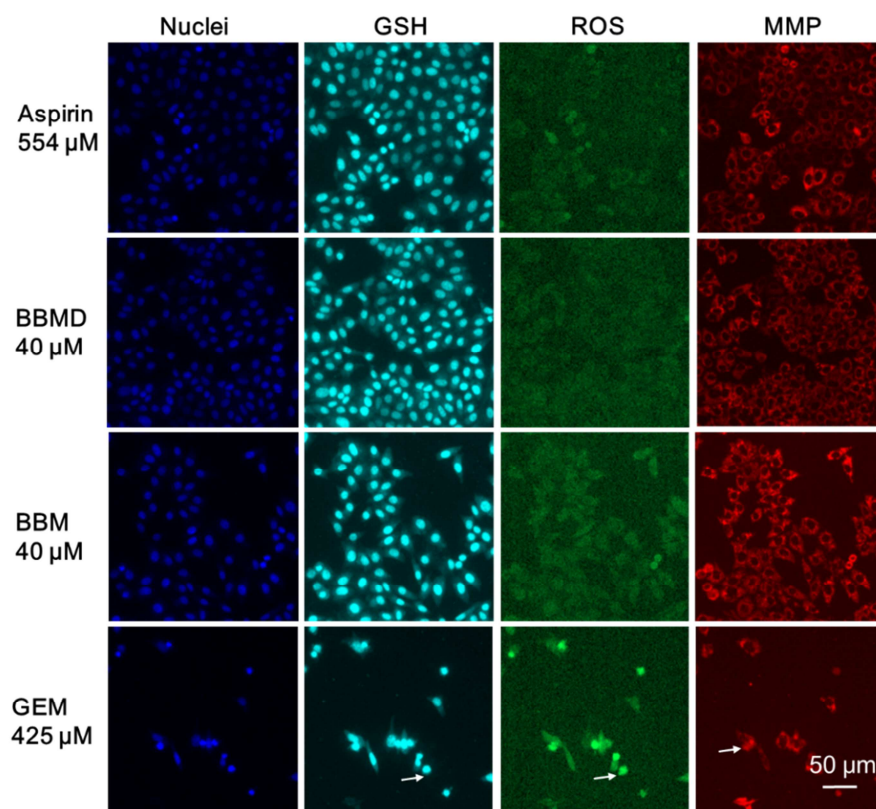
#### *Hepatotoxicity evaluation of BBM and BBMD*

To assess the potential hepatotoxic effects of BBM and BBMD, we undertook *in vitro* DILI assays using HepG2 cells. Fluorescence images of nuclei, GSH, ROS, and MMP in HepG2 cells were captured on four channels (Fig. 5A). Sensitivity and specificity of the assays were 100% as determined by the ToxInsight DILI assay. Toxicity thresholds were calculated based on responses to aspirin. GEM (positive control) induced obvious cell loss, DNA condensation, GSH depletion, ROS formation, and MMP alteration. BBMD did not induce remarkable phenotypic alteration of HepG2 cells, whereas BBM decreased cell number slightly, induced DNA condensation, promoted GSH

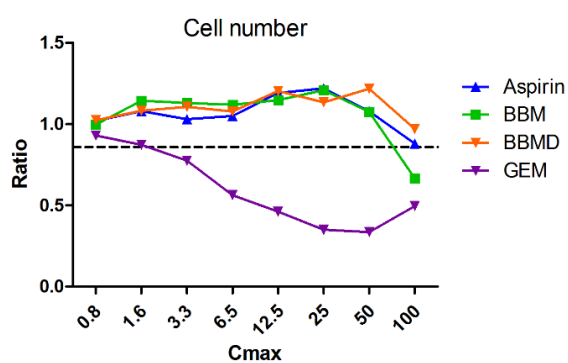


and ROS formation, and altered the MMP response (Fig. 5B–F). These data suggested that BBMD may be less hepatotoxic than BBM.

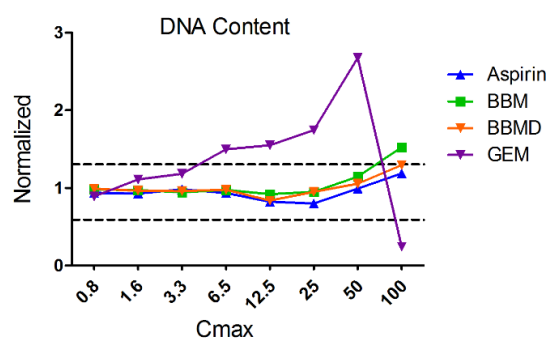
A



B



C



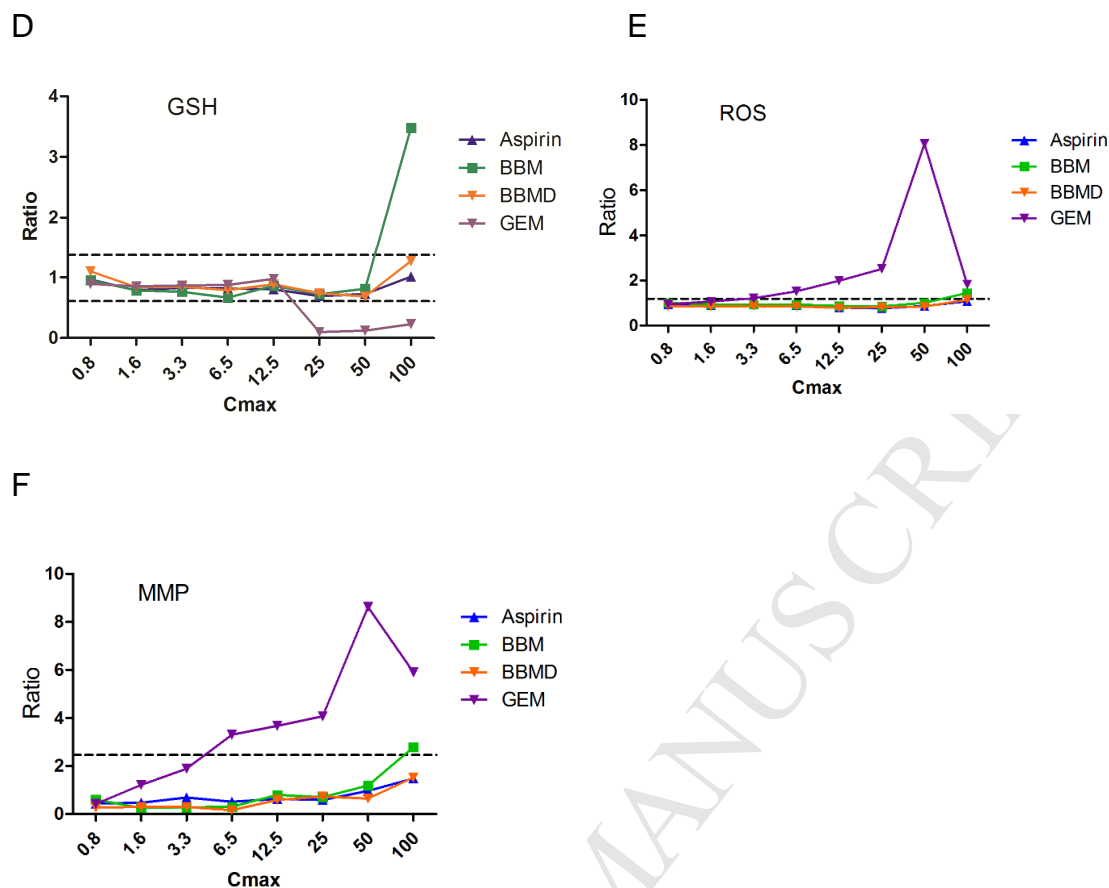


**Figure 5** Evaluation of the hepatotoxicity of berbamine (BBM) and berbamine dihydrochloride (BBMD).

(A) Fluorescence images of HepG2 cells. Nuclei, reduced glutathione (GSH), intracellular reactive oxygen species (ROS), and the mitochondrial membrane potential (MMP) were stained with a ToxInsight™ DILI Assay Cartridge. Cells were incubated with 554  $\mu$ M aspirin, 425  $\mu$ M gemfibrozil, 40  $\mu$ M berbamine (BBM), or 40  $\mu$ M berbamine dihydrochloride (BBMD). Test compound-induced responses were normalized to that of the vehicle control. Dashed lines denote toxicity thresholds determined based on the mean response and standard deviation (SD) of aspirin:  $T = \text{mean} \pm 3 \times \text{SD}$ . Scale bar = 50  $\mu$ m. For cell number (B), responses below the threshold were defined as “toxic”; for DNA content (D),

GSH (D), and MMP (F), responses outside the bidirectional dashed lines were denoted as toxic; for ROS (E), responses above the dashed lines were denoted as toxic. Data are the mean of three independent experiments.

Euclidean distance and angle were applied to determine the extent of hepatotoxicity based on five representative biomarkers. A single dose point of BBM exceeded the threshold constructed by the angle and Euclidean distance, so it was denoted as “toxic”. Dose plots of BBMD were within thresholds so BBMD was denoted as “non-hepatotoxic” (Fig. 6A). Furthermore, we ranked the responses to liver toxicity based on a triangular area constructed by the maximum Euclidean distance and angle. GEM showed the strongest hepatotoxicity and was ranked number one. BBM was ranked number two and its response was much weaker than that of GEM. BBMD was quite similar to the negative control (aspirin) (Fig. 6B). These data further confirmed that BBMD was free of toxicity within the concentrations tested.

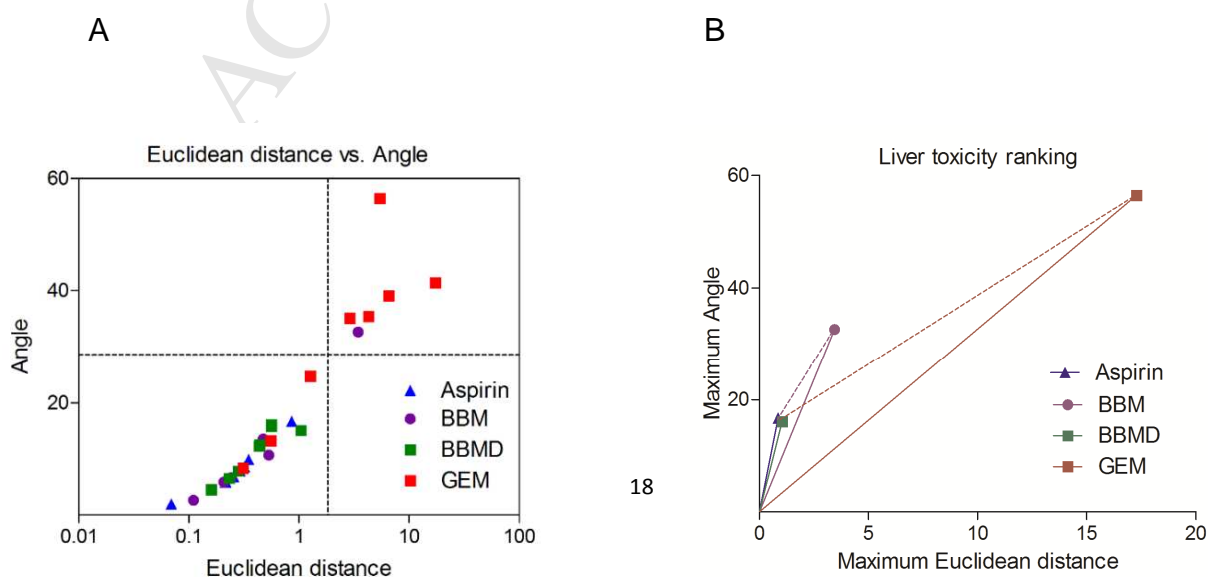


**Figure 6** Determination of hepatotoxicity for test compounds using the Euclidean distance and angle.

(A) Test compounds with points outside the thresholds were defined as “toxic”. (B) Ranking of compounds that induced hepatotoxicity was based on the maximum Euclidean distance and angle. The longer the Euclidean distance and the larger the angle, the stronger the hepatotoxicity.

## Discussion

BBM is a natural bisbenzylisoquinoline alkaloid isolated mainly from the root of the TCM barberry (*Berberis vulgaris* L.). BBM content in barberry ranges from 1.59% to 3.67% depending on geographic distribution in China.<sup>21,22</sup> BBMD is a dihydrochloride derivate of BBM. This is the first study to report the inhibitory effects of BBM and BBMD on adipocyte differentiation and LD deposition.

Studies have shown that BBM possesses various biologic properties. Xu et al.<sup>23</sup> found that BBM exhibited anti-leukemia activity by inhibiting expression of the bcr/abl fusion gene. Other studies have shown that BBM can induce

inhibition of proliferation of liver tumors by targeting  $\text{Ca}^{2+}$ /calmodulin-dependent protein kinase II (CAMKII).<sup>24,25</sup> Investigations on the effects of BBM on cancer cells have also been carried out. Research by Wang et al.<sup>26</sup> suggested that BBM inhibited proliferation of HepG2 cells ( $\text{IC}_{50} \approx 35 \mu\text{M}$ ) and induced apoptosis of HepG2 cells. Wei *et al.*<sup>27</sup> demonstrated that BBM inhibited chronic myelogenous leukemia cell growth by up to  $20 \mu\text{M}$ . However, cytotoxicity may be weakened if BBD is transformed into BBMD. Fang et al.<sup>28</sup> suggested that O-4-ethoxyl-butyl-berbamine (a derivative of BBM) reversed liver toxicity induced by doxorubicin and pegylated doxorubicin. The present study suggests that BBM and BBMD suppressed LD accumulation at relatively low doses ( $<10 \mu\text{M}$ ) without obvious cell injury but that increases in concentration could increase the risk of adverse reactions.

Our findings suggest that BBMD could be applied against infection by the hepatitis-C virus (HCV) and *Mycobacterium tuberculosis*. LDs are important in the assembly and replication of the HCV.<sup>29,30</sup> Thus, LD depletion may reduce the stability of the HCV core and facilitate HCV treatment. In the latency period of infection by *M. tuberculosis*, LDs serve as energy sources for *M. tuberculosis* persistence.<sup>31</sup> Therefore, BBMD may provide a therapeutic approach for HCV infection and tuberculosis through its ability to inhibit LD formation. Nonetheless, the underlying molecular mechanism elucidating how BBM and BBMD regulated adipocyte differentiation demands further investigation. Still, drug induced liver injury assay *in vitro* we employed was

dependent on the C<sub>max</sub> value of test drug. Meanwhile, the C<sub>max</sub> values of BBM and BBMD were currently not accurately determined, which may somewhat influence the accuracy of prediction.

## Conclusions

In summary, the current study developed a high content image-based assay incorporating lipid droplet analysis and drug induced liver injury, which meets the demand for high throughput anti-adipogenic agent discovery. We identified BBM and BBMD from a library of TCM compounds as inhibitors of LD formation in 3T3-L1 adipocytes. By comparing their efficacies and potential hepatotoxic responses, BBMD was found to exert superior bioactivity and weaker adverse effects than BBM. Our discovery of a novel regulator of LD metabolism could provide an alternative avenue for treatment of lipid-associated diseases.

## Acknowledgment

This work was supported by a grant from the National Natural Science Foundation of China (grant number 81430094).

### Author contributions

Shifeng Wang conducted the main experiments and wrote the manuscript. Qiao Zhang and Qinghua Wu undertook imaging analyses. Yanling Zhang and Yuxin Zhang provided writing assistance. Yanjiang Qiao and Shiyu Li designed the study.

### Conflicts of interest

The authors report no conflict of interest.

### References

1. Guo Y, Cordes KR, Farese RV, Walther TC. Lipid droplets at a glance. *J Cell Sci.* 2009;122:749-752.
2. Kuerschner L, Moessinger C, Thiele C. Imaging of lipid biosynthesis: how a neutral lipid enters lipid droplets. *Traffic.* 2008;9:338-352.
3. Barneda D, Frontini A, Cinti S, Christian M. Dynamic changes in lipid droplet-associated proteins in the “browning” of white adipose tissues. *Biochim Biophysica Acta.* 2013;1831:924-933.
4. Kiss E, Kränzlin B, Wagenblaß K, et al. Lipid droplet accumulation is associated with an increase in hyperglycemia-induced renal damage: prevention by liver X receptors. *Am J Pathol.* 2013;182:727-741.
5. Tirinato L, Liberale C, Di Franco S, et al. Lipid droplets: a new player in colorectal cancer stem cells unveiled by spectroscopic imaging. *Stem*

- Cells*. 2015;33:35-44.
6. Gregoire FM, Smas CM, Sul HS. Understanding adipocyte differentiation. *Physiol Rev*. 1998;78:783-809.
  7. Nawrocki AR, Scherer PE. Keynote review: the adipocyte as a drug discovery target. *Drug Discov Today*. 2005;10:1219-1230.
  8. Dragunow M, Cameron R, Narayan P, O'Carroll S. Image-based high-throughput quantification of cellular fat accumulation. *J Biomol Screen*. 2007;12:999-1005.
  9. Spandl J, White DJ, Peychl J, Thiele C. Live cell multicolor imaging of lipid droplets with a new dye, LD540. *Traffic*. 2009;10:1579-1584.
  10. Michaut A, Moreau C, Robin MA, Fromenty B. Acetaminophen-induced liver injury in obesity and nonalcoholic fatty liver disease. *Liver Int*. 2014;34:171-179.
  11. Xia M, Huang R, Witt KL, et al. Compound cytotoxicity profiling using quantitative high-throughput screening. *Environ Health Perspect*. 2008;116:284-291.
  12. Jetten MJ, Kleinjans JC, Claessen SM, Chesne C, Van Delft JH. Baseline and genotoxic compound induced gene expression profiles in HepG2 and HepaRG compared to primary human hepatocytes. *Toxicol In Vitro*. 2013;27:2031-2040.
  13. O'Brien PJ, Irwin W, Diaz D, et al. High concordance of drug-induced human hepatotoxicity with in vitro cytotoxicity measured in a novel



- cell-based model using high content screening. *Arch Toxicol.* 2006;80:580-604.
14. Suh HJ, Cho SY, Kim EY, Choi HS. Blockade of lipid accumulation by silibinin in adipocytes and zebrafish. *Chem Biol Interact.* 2015;227:53-62.
  15. Zhao J, Zhu H, Wang S, et al. Naoxintong protects against atherosclerosis through lipid-lowering and inhibiting maturation of dendritic cells in LDL receptor knockout mice fed a high-fat diet. *Curr Pharm Des.* 2013;19:5891-5896.
  16. Fu F, Tian F, Zhou H, et al. Semen cassiae attenuates myocardial ischemia and reperfusion injury in high-fat diet streptozotocin-induced type 2 diabetic rats. *Am J Chin Med.* 2014;42:95-108.
  17. Zhang Z, Zhang H, Li B, et al. Berberine activates thermogenesis in white and brown adipose tissue. *Nat Commun.* 2014;5:5493.
  18. Wang S, Zhai C, Liu Q, et al. Cycloastragenol, a triterpene aglycone derived from *Radix astragali*, suppresses the accumulation of cytoplasmic lipid droplet in 3T3-L1 adipocytes. *Biochem Biophys Res Commun.* 2014;450:306-311.
  19. Zhang J, Chung TD, Oldenburg KR. A simple statistical parameter for use in evaluation and validation of high throughput screening assays. *J Biomol Screen.* 1999;4:67-73.
  20. Nishio E, Tomiyama K, Nakata H, Watanabe Y.

- 3-Hydroxy-3-methylglutaryl coenzyme A reductase inhibitor impairs cell differentiation in cultured adipogenic cells (3T3-L1). *Eur J Pharmacol.* 1996;301:203-206.
21. Lu GH, Chen JM, Xiao PG. Determination of alkaloids in the roots of Berberis genus plants by HPLC with varied wavelength. *Acta Pharmaceutica Sinica.* 1995;30:280-285. [Chinese]
22. Di DL, Wang Q, Ma ZG, Jiang SX. Distribution of four alkaloids in plants of Berberis. *Journal of Chinese Medicinal Materials.* 2004;27:83-86. [Chinese]
23. Xu R, Dong Q, Yu Y, et al. Berbamine: a novel inhibitor of bcr/abl fusion gene with potent anti-leukemia activity. *Leuk Res.* 2006;30:17-23.
- [24. Meng Z, Li T, Ma X, et al. Berbamine inhibits the growth of liver cancer cells and cancer-initiating cells by targeting Ca<sup>2+</sup>/calmodulin-dependent protein kinase II. *Mol Cancer Ther.* 2013;12:2067-2077.
25. Gu Y, Chen T, Meng Z, et al. CaMKII gamma, a critical regulator of CML stem/progenitor cells, is a target of the natural product berbamine. *Blood.* 2012;120:4829-4839.
26. Wang GY, Lü QH, Dong Q, Xu RZ, Dong QH. Berbamine induces Fas-mediated apoptosis in human hepatocellular carcinoma HepG2 cells and inhibits its tumor growth in nude mice. *J Asian Nat Prod Res.* 2009;11:219-228.
27. Wei YL, Xu L, Liang Y, Xu XH, Zhao XY. Berbamine exhibits potent

antitumor effects on imatinib-resistant CML cells in vitro and in vivo.

*Acta Pharmacol Sin.* 2009;30:451-457.

28. Fang BJ, Yu ML, Yang SG, Liao LM, Liu JW, Zhao RC. Effect of O-4-ethoxyl-butyl-berbamine in combination with pegylated liposomal doxorubicin on advanced hepatoma in mice. *World J Gastroenterol.* 2004;10:950-953.
29. Miyanari Y, Atsuzawa K, Usuda N, et al. The lipid droplet is an important organelle for hepatitis C virus production. *Nat Cell Biol.* 2007;9:1089-1097.
30. Filipe A, McLauchlan J. Hepatitis C virus and lipid droplets: finding a niche. *Trends Mol Med.* 2015;21:34-21.
31. Neyrolles O, Hernandez-Pando R, Pietri-Rouxel F, et al. Is adipose tissue a place for Mycobacterium tuberculosis persistence? *PLoS One.* 2006;1:e43.